



Estimating crop coefficients for pistachios and grapes using SEBAL and simple reference evapotranspiration methods in the Central basin of Iran

Hossein Malakinezhad¹ · Fatemeh Firoozi¹ · Kamran Rahimi²

Received: 20 September 2021 / Accepted: 17 September 2022 / Published online: 29 September 2022
© Saudi Society for Geosciences 2022

Abstract

Water is a key limiting factor for agricultural production in the arid and semiarid regions of Iran that are experiencing a recent decline in rainfall and groundwater level. Under such challenges, the efficient use of available water with an accurate knowledge of crop water requirement is crucial to maintain Iran's agricultural production. While crop water use or evapotranspiration (ET) modeling offers an opportunity to assist crop water-saving interventions by providing useful information on crop water stress and availability, such applications are challenging in Iran due to limited data availability. In this study, we used a remote sensing approach coupled with surface energy balance algorithm for land (SEBAL) to estimate regional-scale ET and crop coefficient (i.e., K_c, the ratio of actual ET to reference ET) from pistachio and grape dominated fields in the Central basin of Iran. The primary objective of the study is to assess the ability of 11 less-data intensive and simple reference crop evapotranspiration methods, namely FAO PM, Trajkovic, Irmak, Bereti, Blaney-Criddle, Rozani, Rn-Based, Trabert, Tabari and Droogers–Allen and Hargreaves–Samani (H–S) methods, to derive crop coefficients when coupled with remote sensing-based SEBAL model. Crop coefficients derived from these models were compared with those derived from widely approved Penman–Monteith (FAO P–M) method that typically requires a lot of meteorological data including wind speed, radiation, temperature, and relative humidity. Crop coefficients derived from the 11 reference ET models for the months of August, November, February, and May in the year 2017 varied widely. Among the 11 reference ET models, we found H–S, Blaney–Criddle, and Trabert models produced crop coefficients close to those from the FAO PM method. On the other hand, Trajkovic, Bereti, and Rozani methods were found to be not applicable, especially in August and May. The root mean squared error (RMSE) values between crop coefficients from the simple reference ET models FAO PM method suggested H–S Blaney–Criddle and Trabert may be applicable for 4 months. Overall, the majority of reference ET models produced unrealistic values of K_c due to significant underestimation of reference ET. This study provides useful guidance on the simple reference crop methods for understanding water requirements of pistachio and grape in the Central basin of Iran in case of limited data availability.

Keywords Crop coefficients · Evapotranspiration · Empirical methods · MODIS · SEBAL

Introduction

Water is considered as the most critical resource for sustainable development in many countries (Chartzoulakis and Bertaki 2015). In the arid and semiarid regions, water is a limiting factor for agricultural production (Dehghanisanij et al. 2006) and the unsustainable use of water coupled with extreme climatic events such as frequent droughts have challenged agricultural water management in these regions. Proper management of agriculture and water resources with a better understanding of crop water use is critical to help conserve water, promote sustainable production practices,

Responsible Editor: Biswajeet Pradhan

✉ Hossein Malakinezhad
hmalakinezhad@yazd.ac.ir

Fatemeh Firoozi
firozif@yahoo.com

Kamran Rahimi
kamranrahimi30@yahoo.com

¹ Faculty of Natural Resources, Yazd University, Yazd, Iran

² Kharazmi University, Tehran, Iran

and optimize irrigation management (Rahimzadegan and Janani 2019).

Evapotranspiration combines water losses to the atmosphere through soil evaporation and vegetation transpiration, and represents the second most important component in the assessment of the hydrological cycle (Brutsaert 2005).

One of the important parameters in this regard is the determination of evapotranspiration (ET) from crops that varies widely across species and growth stages, geographical regions, climate, and time (Rahimzadegan and Janani 2019). ET involves evaporation from the soil surface and transpiration from vegetation and is considered a fundamental process to balance Earth's energy and water cycles (Yamaç and Todorovic 2019; Yang et al. 2018; Jensen 1968). ET information is key for sustainable water resources management, especially in arid and semi-arid regions (Gao et al. 2008, 2019). The most common method of calculating ET includes field methods, such as lysimeter, eddy covariance, scintillometer. However, these methods are labor- and cost-intensive. Another widely used method is the use of crop coefficients (K_c , the ratio of actual to reference ET) and reference ET based on the Penman–Monteith FAO 56 equation (Cai et al. 2007). In addition, these methods (field based and crop coefficient based models) can only estimate ET at a point scale and only applicable for homogenous area covering a single crop. Hence, these methods are not applicable for large-scale applications such as the derivation of basin scale ET due to the dynamic nature and regional variations of ET. As such, these methods alone are not suitable for applications in understanding crop water use across a large scale, often a requirement in sustainable water management. Another disadvantage of the PM FAO-56 equation is that it requires detailed meteorological data, which is not always available in many regions across the globe (Gocic and Trajkovic 2010; Tabari and Hosseinzadeh Talaei 2011; Tabari et al. 2011). For this reason, to accurately estimate the ET and water requirements of plants, it may be possible to use simple experimental methods that require less data (Piri and Taher 2019). Some of these include Irmak, Tabari, Trajkovic, Bereti, Blaney Criddle, Rozani, Rn Based, and Droogers – Allen (Tabari and Hosseinzadeh Talaei 2011; Piri and Taher 2019). A key measure of crop water requirement is the ratio of actual to reference ET or the crop coefficient (K_c) (Allen et al. 1998), which varies across crops and seasons. Reference ET which is the potential rate of ET from a hypothesized crop such as alfalfa or clipped grass at reference height (0.12 cm) (Allen et al. 1998). Increasing demand for crop production to sustain a growing population has exerted pressure on available water resources to increase production with limited resources (Ray et al. 2013). The global average the rate of water abstraction for irrigation has increased by 60% since 1960, of which 20–30% was lost through ET (Bates et al. 2008). International Water

Management Institute (IWMI) analyzed two different global theories for the production of different products and food supply in 2001. First, the water allocated to agriculture is insufficient to supply the world's poor foodstuffs, and the possibility of extracting more water from surface and underground sources is at most 11–12%. A wide range of new technologies and strategies have been adopted to optimize the use of agricultural water (Bates et al. 2008). A significant advancement in remote sensing application in agricultural water management includes development of several thermal remote sensing based surface energy balance (SEBS) algorithms over the last few decades (Anderson et al. 2008): The surface energy balance system (SEBS, (Su 2002)), surface energy balance algorithm for land (SEBAL, (Bastiaanssen et al. 1998)), Surface Energy Balance Index (SEBI (Menenti and Choudhury 1993)), and Mapping Evapotranspiration at high Resolution with Internalized Calibration (METRIC (Allen et al. 2007)). Among these, SEBAL is one of the most widely used models that can estimate with minimal meteorological and remotely sensed data using empirical and physical relationships (Bastiaanssen et al. 1998). SEBAL model has been widely validated across the globe (Bhattarai et al. 2016; Bhattarai and Liu 2019). SEBAL accuracy is considered to be 85% at a daily scale that can increase up to 95% at a seasonal scale (Bastiaanssen et al. 2005). While these accuracies have been contested in several studies, SEBAL is widely considered as one of the most widely regarded SEBAL models. Though initially designed for Landsat, SEBAL has been widely implemented on MODIS (Moderate Resolution Imaging Spectroradiometer) for regional scale ET monitoring (Bashir Mohammed et al. 2010; Tang et al. 2013; Bhattarai et al. 2012, 2019). SEBAL has also been used to compute (K_c) to estimate the crop water requirements (Islam 2004; Li et al. 2008; Rawat et al. 2017; Bashir Mohammed et al. 2010). Rahimzadegan and Janani (2019) implemented SEBAL model on pistachio in Semnan during 2013–2017 using 29 images of Landsat 8. The result showed high spatial variability of ET in pistachio growth period. In general, the results show that the SEBAL model has a high efficiency for estimating the true ET of pistachio crop. Therefore, real evapotranspiration can be calculated periodically and regularly over a wide range of areas with high reliability. However, the majority of these studies use FAO PM based reference ET that require several meteorological variables (Goldhamer 1995). Applications of the FAO PM reference ET models to derive K_c across the dry and semi-arid plains of Herat and Marvast of Iran are not practical given the limitation of weather networks in these areas. This becomes more challenging to derive spatial distribution of K_c values across these regions that are dominated by high value crops like pistachio and grape orchards. Though these crops are known to being drought tolerant, irrigation is critical for maintaining their growth and yield (Bellvert et al.

2018). Little research has been carried out in the field of satellite estimates of ET on pistachio and grapes ET product, which are the most important agricultural products of Iran.

The purpose of this study is to investigate the utility of twelve experimental reference ET methods that require minimum meteorological data and the SEBAL model to estimate the water requirements of pistachio and grape orchards in the dry and semi-arid plains of Herat and Marvast. The main objective is to identify the best experimental reference ET methods that can produce Kc values for these crops similar to those produce by the FAO P–M method in this region. Finally, the water requirement of pistachio and grape crops in the study area is calculated, and the findings of this study will provide useful information for agricultural water management in the arid region of Herat and Marvast.

Materials and methods

Study area

The plain of Herat and Marvast is located at the main central basin of Iran (Mazidi and Barzegar Marvasti 2016) (Fig. 1). The dominant crops of this plain are pistachio and grape. The average annual rainfall is about 100 mm and it ranges up to 250 mm in some mountainous areas. The annual ET is typically about 15 to 20 times the annual rainfall. Deep and

semi-deep wells are extensively used to irrigate pistachio and grape orchards (Moghimi and Zare Abadi Iqbal 2014).

Data

The key inputs of the SEBAL model include remotely sensed biophysical parameters, such as land surface temperature (LST or Ts), emissivity, normalized difference vegetation index (NDVI), and albedo in addition to hourly meteorological parameters, such as air temperature, wind speed, radiation, and relative humidity. In this paper, MODIS sensor radiance data product (MOD021KM) and meteorological stations at Herat and Marvast were used to provide the remote sensing and meteorological inputs, respectively. MODIS LST product was extended to the whole globe from the arctic region to the South Pole and at least one site for every continent (Wan 2014). The normalized difference of the vegetation index (NDVI) was calculated as:

$$NDVI = \frac{B2 - B1}{B2 + B1} \tag{1}$$

where B1 and B2 are surface reflectance from near infrared (NIR) and red bands of the MOD021KM products. Surface albedo (α) was obtained using band specific weighted values from (Li et al. 2008), where α_1 to α_7 are the reflectance rates of the first to seventh channel of MODIS data.

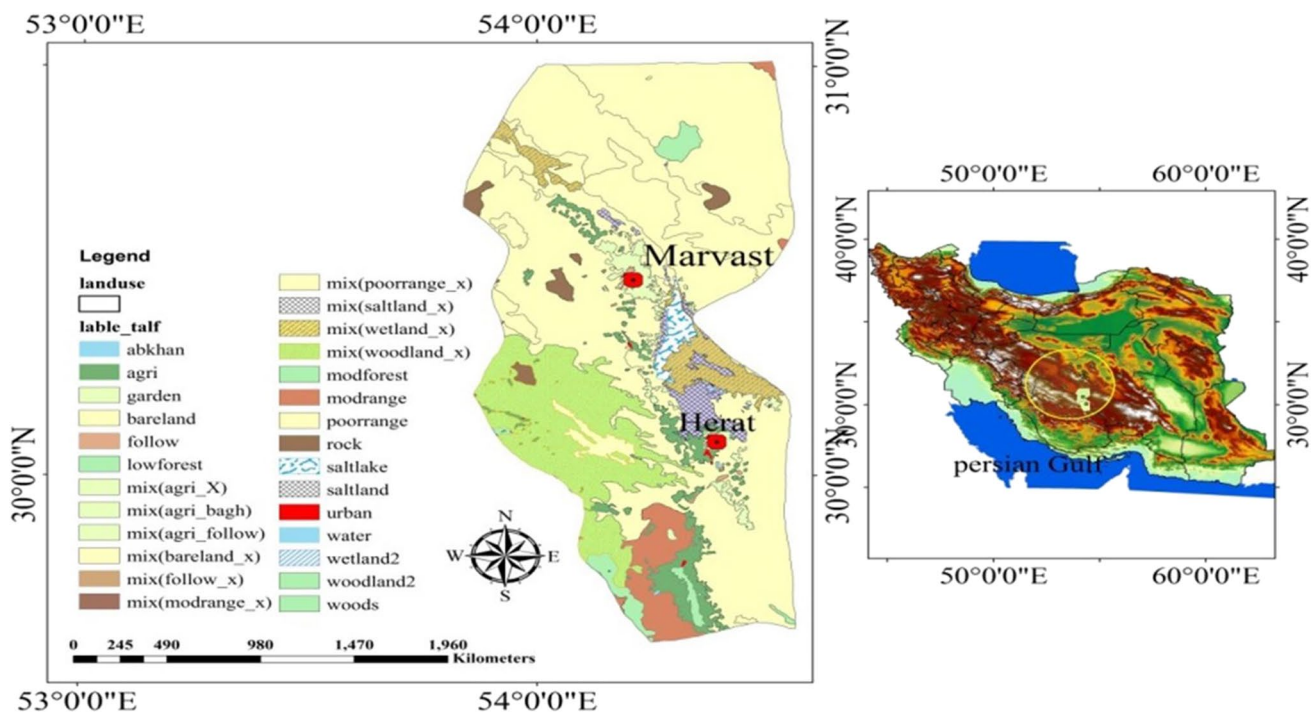


Fig. 1 The geographical location of the study area

$$\alpha = 0.160_{\alpha1+} 0.291_{\alpha2+} 0.243_{\alpha3+} 0.116_{\alpha4+} 0.112_{\alpha5+} 0.081_{\alpha7-} 0.0015 \quad (2)$$

Methods

ET estimation using SEBAL model

The general equation of the surface energy balance (SEB) is solved in the SEBAL model with latent heat flux (λET , Wm^{-2}) as a residual of the SEB. λET is the energy term of the ET, where λ is the latent heat of vaporization, Jkg^{-1} .

$$\lambda ET = Rn - G - H \quad (3)$$

where λET is the latent heat flux (W/m^2), Rn is the net radiation flux at the surface (W/m^2), G is the soil heat flux (W/m^2), and H is the sensible heat flux (W/m^2) (Bastiaanssen et al. 1998; Rahimzadegan and Janani 2019)

$$Rn = (1 - \alpha)R_{s\downarrow} + R_{L\downarrow} - R_{L\uparrow} - (1 - \epsilon_0)R_{L\downarrow} \quad (4)$$

In it Rn : total radiation flux in terms of $R_{s\downarrow}$ (W/m^2) shortwave radiation, α surface albedo without dimension, $R_{L\downarrow}$ longwave radiation, $R_{L\uparrow}$ long wave reflection, ϵ_0 ability to propagate surface without dimension. The equations for deriving each component of the radiation balance are provided in (Allen et al.1998). Soil heat flux (G) is computed using the empirical equation from (Bastiaanssen et al.1998).

$$[G = \frac{T_s - 273.15}{\alpha(0.0038\alpha + 0.0074\alpha^2)(1 - 0.98NDVI^4)} \times R_n] \quad (5)$$

T_s : Surface temperature in degrees Celsius, α : Surface albedo, NDVI: Vegetation index.

Similar to most SEBAL model, H derivation is the most challenging task in the SEBAL model because of the uncertainties associated with aerodynamic temperature and conductance that can be measured directly and more specifically,

the hot and cold extremes that requires human intervention. SEBAL uses a hot (dry, uncultivated farmland) and cold (well-vegetated, well-irrigated area) pixel based approach to internally calibrate H by assuming the linear relationship between near-surface temperature difference (dT) and LST . The internal calibration establishes two extreme ends of H ($H=0$ for cold pixel and $H=Rn-G$ for hot pixel) and LE ($LE=0$ for hot pixel and $LE=Rn-G$ for cold pixel) and the initial dT values are used to update and iterate H by solving equations for aerodynamic resistance r_{ah} , friction velocity (u^*), and stability correction factors.

$$H = \frac{\rho \times c_p \times dT}{r_{ah}} \quad (6)$$

$$r_{ah} = \frac{1}{Ku_*} \left[\ln \left(\frac{z - d_0}{z_{0h}} \right) - \psi_{h(z-d_0)} + \psi_{h(z_{0h})} \right] \quad (7)$$

$$u_* = \frac{ku_b}{\ln \left(\frac{z_b}{z_{0m}} \right) - \psi_{m(z_b)}} \quad (8)$$

where ρ is air density ($kg\ m^{-3}$); c_p is air specific heat capacity ($1004\ J/kg/K$); K is Von Karman's constant (0.41); z is the reference height (m); d_0 is the zero-displacement height (m); and u_b is the wind speed (m/s) at blending height z_b (200 m). The z_{0m} is the roughness length (m) for momentum transfer and z_{0h} is the roughness length (m) for heat transfer. The ψ_m and ψ_h are the stability correction for momentum and heat transport, respectively.

The latent heat flux is calculated as the residual of the energy balance equation. Instantaneous evapotranspiration is obtained using Eq. (9).

$$ET_{inst} = 3600 \frac{\lambda ET}{\lambda} \quad (9)$$

Table 1 Equations used empirical methods. All meteorological variables are derived on a monthly scale (sum). Here R_s is the solar radiation in mm/day , T_c is the average monthly temperature in $^\circ C$, R_a

is the radiation, T_s is the average daily air temperature, T_{max} is the maximum monthly temperature, T_{min} is the minimum monthly temperature, P is the sunshine hours (Piri and Taher 2019)

Row	Methods	Equations
1	Hargreaves Samani	$ET_0 = 0.0162R_s (T_c + 17.8)$ (13)
2	Rozani	$ET_0 = 0.408 \times (0.817 + 0.00022z)0.0023Ra(T_{mea} + 17.8)(T_{max} - T_{min})^{0.5}$ (14)
3	Trajkovic	$ET_0 = 0.408 \times 0.0023 Ra (T_{mean} + 17.8)(T_{max} - T_{min})^{0.424}$ (15)
4	Irmak	$ET_0 = 0.408 \times 0.00193 Ra (T_{mean} + 17.8)(T_{max} - T_{min})^{0.5}$ (16)
5	Bereti	$ET_0 = 0.408 \times 0.00193 Ra (T_{mean} + 17.8)(T_{max} - T_{min})^{0.5}$ (17)
6	Blaney-Criddle	$ET_0 = P (0.46 T_{mean} + 8.17)$ (18)
7	Rn-Based	$ET_0 = 0.289 R_s + 0.023 T_{mean} + 0.489$ (19)
8	Trabert	(14) $ET_0 = 0.408 + 0.00193 Ra(T_{mean} + 17.8)(T_{mean} + 17.8) (T_{max} - T_{min})^{0.517}$ (20)
9	Tabari	$ET_0 = ET_0 = -0.642 + 0.174R_s + 0.0353 Ta$ (21)
10	Droogers – Allen	$ET_0 = 0.408 \times 0.0030 Ra (T_{mean} + 17.8)(T_{max} - T_{min})^{0.5}$ (22)

ET_{inst} : Actual evapotranspiration rate (mm/hr), λ : latent heat of vaporization (J/kg) (Waters et al. 2002a).

Evapotranspiration is calculated in 24 h using the evaporative fraction ($\Lambda = LE/(Rn-G)$), assuming the constant throughout the day, for each pixel as:

$$ETd = 86400 * \Lambda * Rn24/\lambda \tag{10}$$

where Rn24 is the 24-h net radiation.

It should also be noted that the selected images were not cloudy in areas where there was vegetation and agricultural land, but if it was cloudy in these areas, using the method of identifying and retrieving areas with cloud cover, in three main stages. In the first stage, cloud pixels and in the second stage, shadow pixels are identified. After identifying these pixels and creating a mask on them, in the third step, their probable values are estimated using the surrounding pixels. In general, the identification of cloud pixels in various researches is done in two main ways. In the first method, the classification is done on the raw

image and in the obtained results and the cloudiness class is identified (Amato et al. 2008).

Monthly ET from SEBAL

Ideally, monthly ET from SEBAL is obtained by running SEBAL model for all days of each month. However, because the thermal bands are highly sensitive to clouds, obtaining LST maps for all days within a given month is nearly impossible. Hence, we linearly interpolated Λ for the missing day and multiplied by Rn24 (Waters et al. 2002b) for the given day to estimate daily ET maps for the missing LST pixels. In this study, we considered four specific months (February, May, August, and November) in the year 2017 to estimate Kc values for pistachio and grape. These four months represent key growth stages of pistachio and grape, as the growing season begins on May, peaks around August, leaves fall and senescence on November, and the crops hibernate on February. All available daily MOD021KM products were

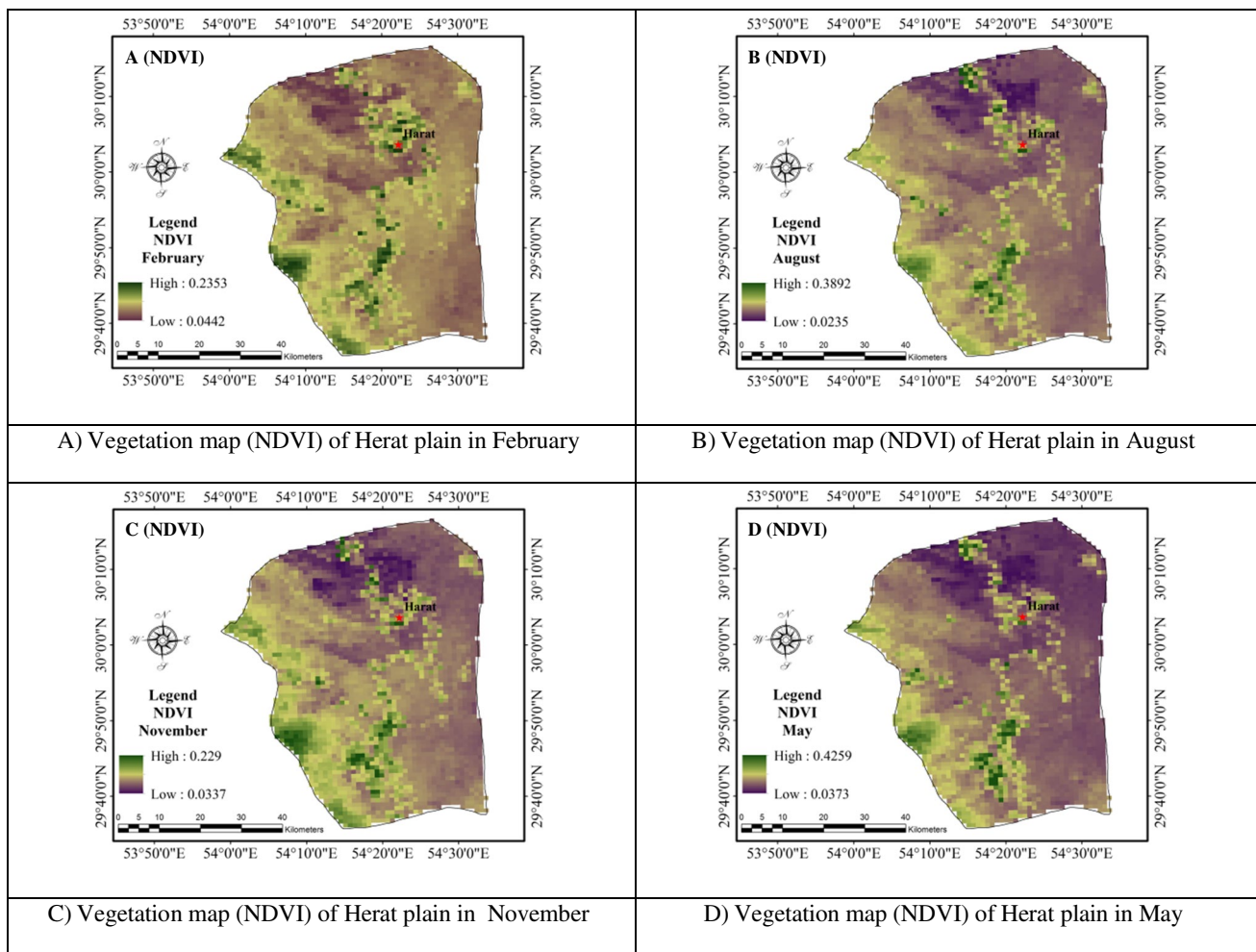


Fig. 2 Vegetation maps (NDVI) of Herat plain in February, August, November, and May for the period 2017

used and missing days/pixels values were interpolated, as described earlier.

Reference ET estimation

FAO-56 Penman–Monteith method

In this study, we considered reference ET for a reference grass condition, which includes a grass height of 0.12 m, surface resistance of 70 s/m, and an α of 0.23. This level is similar to a large green lawn surface, well irrigated with uniform height, with active growth and complete shading (Allen et al. 1998). The Penman–Monteith equation is summarized as Eq. (11):

$$ET_0 = \frac{0.408\Delta(R_n - G) + \gamma[890/(T + 273)]U_2(e_a - e_d)}{\Delta + \gamma(1 + 0.34U_2)} \tag{11}$$

where, ET_0 is the reference crop evapotranspiration (mm / day), T is the average air temperature at a height of 2 m above ground level, U_t is the wind speed at a height of 2 m above ground level (ms^{-1}), $e_a - e_d$ is the vapor pressure deficit (KPa), Δ is the vapor pressure curve slope ($KPaC^{-1}$), γ is the Psychrometric coefficient ($KPaC^{-1}$) (Bastiaanssen et al.1998).

The crop coefficient for grape and pistachio fields in our study was derived using monthly SEBAL ET (ET_{mon}) and monthly ET_0

$$Kc = ET_{mon}/ET_0, mon \tag{12}$$

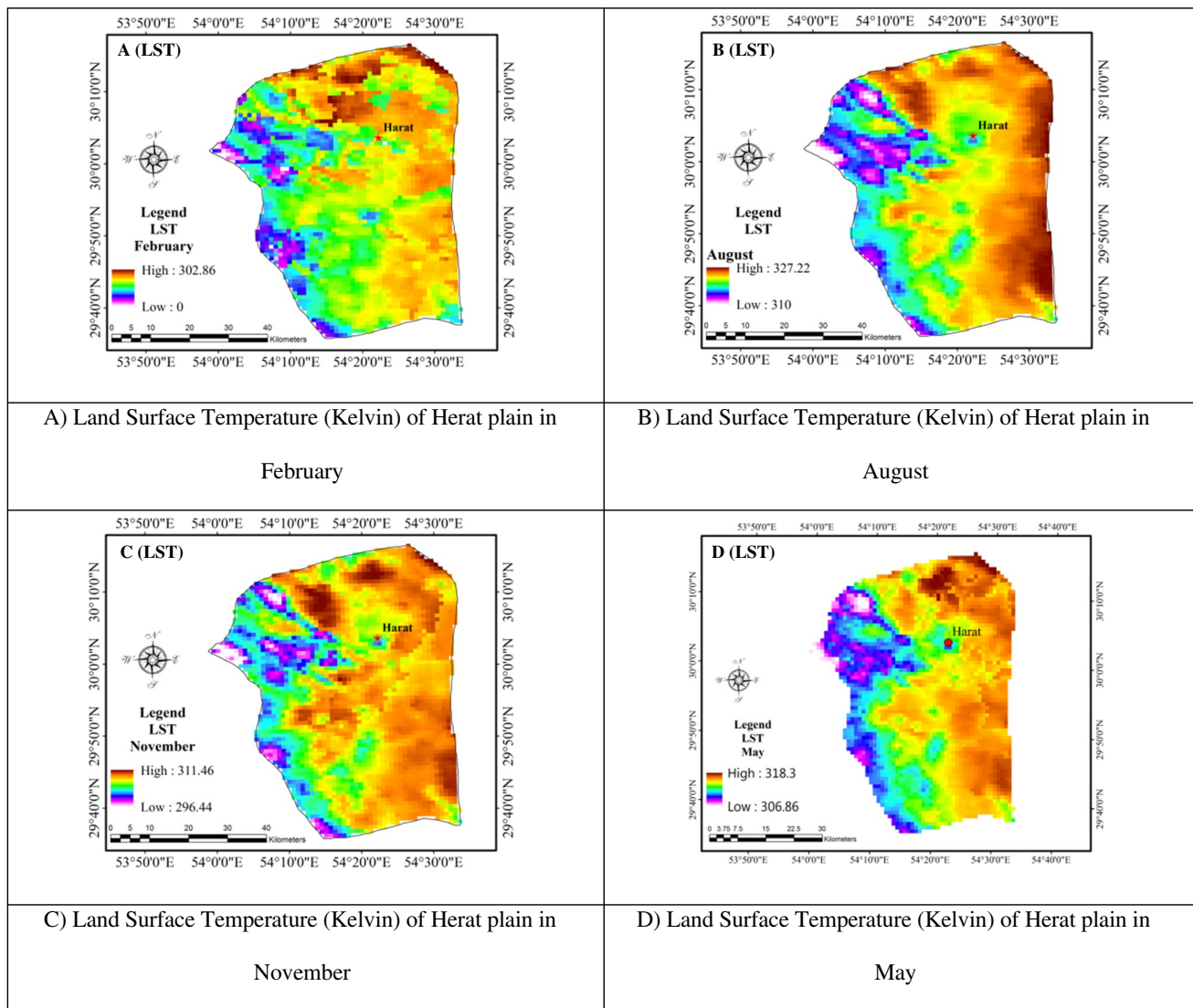


Fig. 3 Land surface temperature (Kelvin) of Herat plain in February, August, November, and May for the period 2017

Empirical methods

Kc from these methods are with those from FAO PM method (Table 1).

After obtaining the Kc from the ten empirical methods, mean absolute error (MAE) and Root Mean Square Error (RMSE) were obtained to determine the average deviation of Kc values from the ten empirical methods with those from the FAO-PM method as:

$$MAE = \frac{1}{n} \sum |K_c(FAO - PM) - K_c(EM)| \tag{23}$$

$$RMSE = \sqrt{\frac{\sum_{i=1}^n (X_i - X_m)^2}{n}} \tag{24}$$

where x_i is evapotranspiration that is calculated using the SEBAL algorithm and x_m is calculated evapotranspiration

using experimental methods and n is the number of evapotranspiration date (Hyndman and Koehler 2006).

Results

Spatio-temporal variation of vegetation and land surface characteristics

NDVI and LST followed consistent patterns across the study and dates (Fig. 2). For example, in Herat plain areas with vegetation cover showed higher NDVI and lower LST values (Figs. 3 and 4). The maximum values of NDVI in pixels in May and August are 0.42 and 0.38, respectively, which is higher than other months due to the beginning of the growing season and the peak of vegetation in both spring and summer. In November and February, NDVI declined due to harvesting and crop

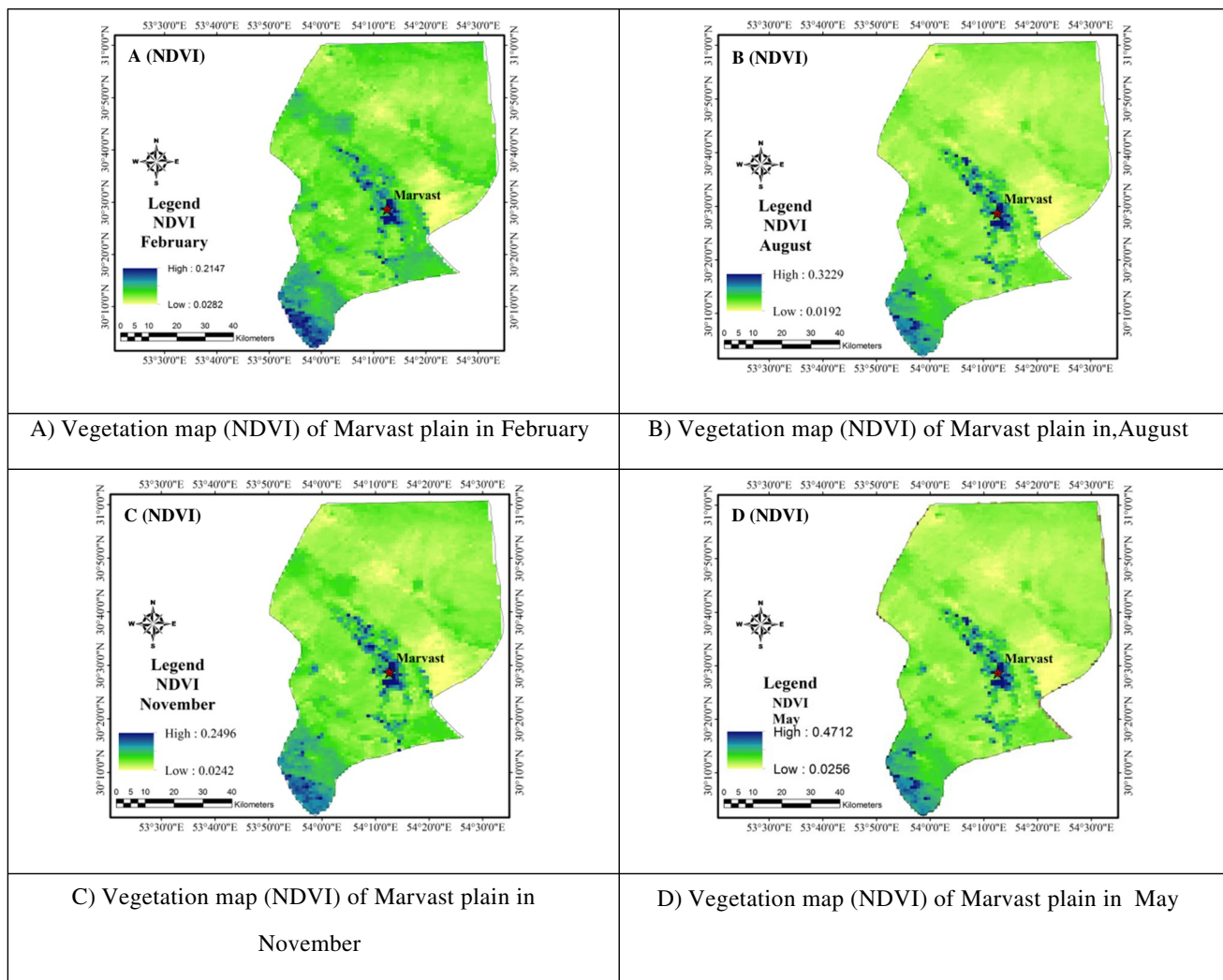


Fig. 4 Vegetation maps (NDVI) of Marvast plain in February, August, November, and May for the period 2017

senescence. The cropped areas were found to have lower surface temperatures due to surface cooling. Mean LST from the cropped areas in February was 290 k, and was much lower than those from the uncultivated lands. LST also followed the seasonal patterns, such as LST values were lower (302 K) in the month of February and higher in the month of August (327.25 K).

In Marvast plain, the maximum values of NDVI in pixels are 0.4, in May which is higher than other months because the growing season begins. In February, NDVI decreased (0.2) due to harvesting and crop senescence (Fig. 4). LST also followed the seasonal patterns, such as LST values were lower (298.36 K) in the month of February and higher in the month of August (331.58 K) (Fig. 5).

Spatial distribution of ET

The spatial distribution of SBEAL ET estimates followed a similar pattern as NDVI and LST (Figs. 6 and 7). ET values were higher for high NDVI and low LST pixels. SEABL-derived monthly ET followed seasonal patterns, as ET values were higher in the spring and summer seasons across the vegetated area for both study regions (Figs. 6 and 7). This is largely due to increased solar radiation and enhanced vegetation growth. ET values were found to be higher in these temperate regions due to the presence of pistachio orchards, arable land, and higher vegetation index in the western and northern parts of the study area. The spatial variability of monthly ET across the study area is due to variations in land use, crop type and date of start of growth and end of the growing season.

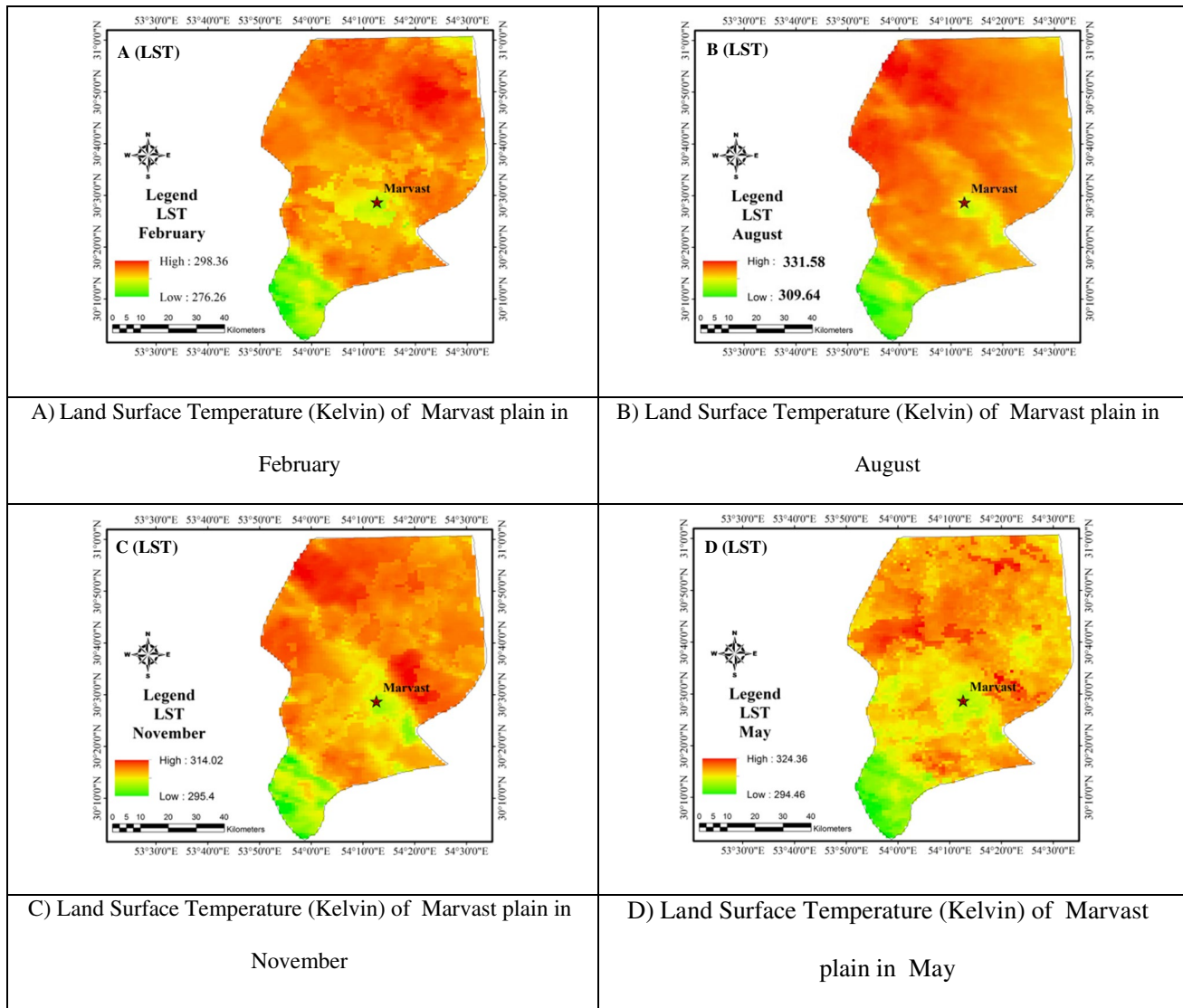


Fig. 5 Land Surface Temperature (Kelvin) of Marvast plain in February, August, November, and May for the period 2017

Monthly SEBAL ET was found to be maximum during the peak growing season (i.e., August) at around 582 mm, when the vegetation reached its maximum greenness (NDVI=0.38). After peak growing season, ET values decreased in November and February with decreasing plant density and decreasing temperature and reduced demand for water. The potential ET from different empirical models was used to analyze the water requirement of grape in the Marvast region and pistachio in the Herat region. Persistent cloud cover in month of February limited derivation of monthly ET for over 20% of study region in the month of February (Fig. 7).

Potential ET from FAO-PM and empirical methods

PET from the ten empirical methods showed wide variation with much lower values compared to the FAO- PM model

(Fig. 8). Though the temporal pattern was similar, as values from most models were maximum during the month of August. The variations between FAO PM and the other PET methods were higher during the months of August and November, also PET from the empirical models were significantly lower than those from the FAO PM method. In most cases, the highest rate of PET was yielded by the FAO PM method. For the month of August, the key irrigation season, FAO PM method estimated PET was 391 mm, which was most closely matched by the H-S method (224 mm) that was still 43% less than the FAO PM PET. Similarly, empirical method derived ET₀ rates in the month of November were significantly lower than those from the FAO PM method. The estimated ET using most models were lowest during the February, and results of the Blaney-Criddle and Trabert methods were most closely matched with FAO PM

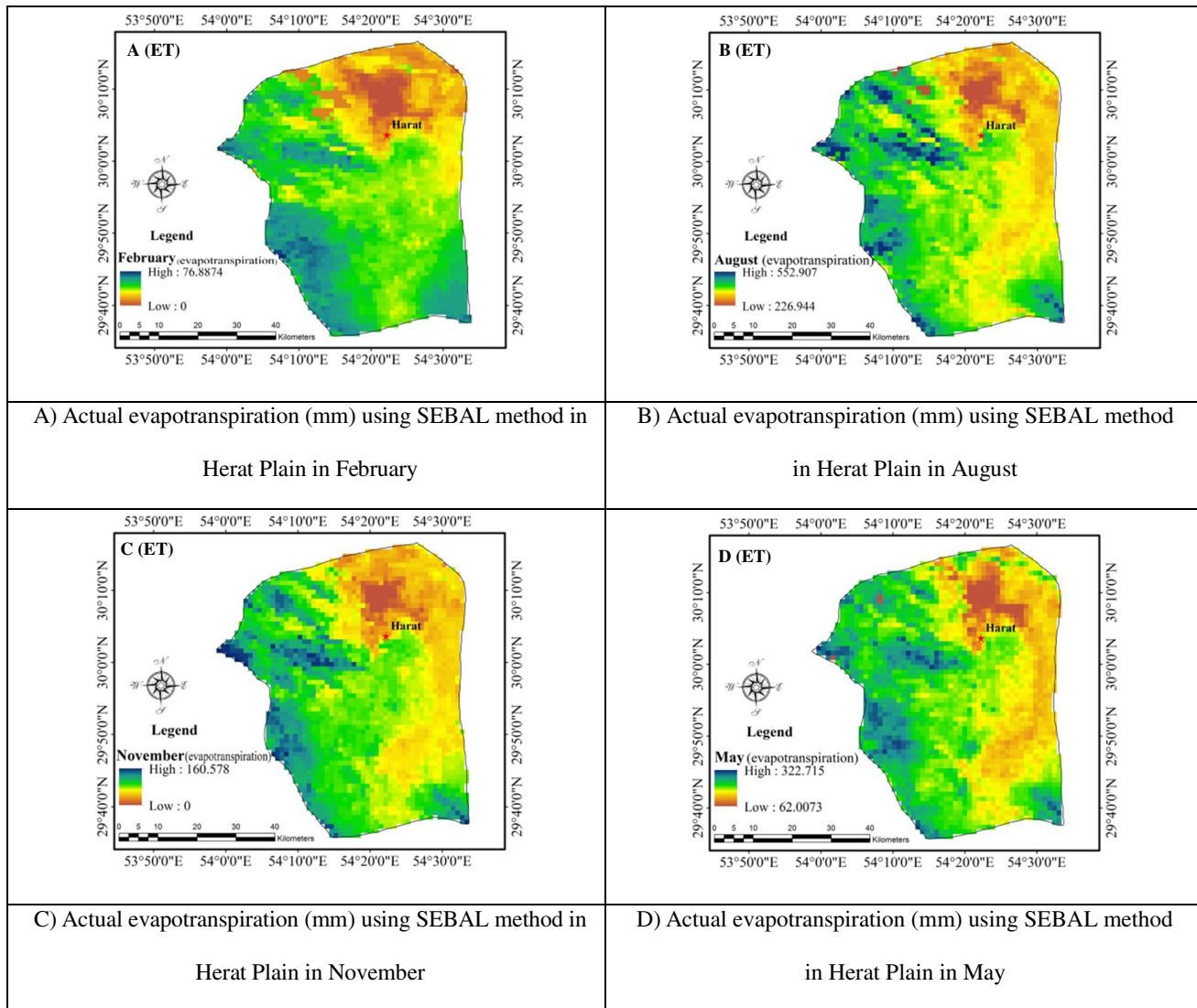


Fig. 6 Actual evapotranspiration (mm) using SEBAL method in Herat Plain in February, August, November, and May for the period 2017

method in the Marvast plains. During the month of May, the H–S derived values were closest to those from the FAO PM method.

The difference between actual monthly ET from SEBAL and the PET from FAO PM algorithm were maximum (161.46 mm) and minimum (39.29) in the month of August and February, respectively. This pattern was consistent across all models; however, the difference between actual and potential ET was much larger in the month of August (e.g., 329.18 mm from H–S method and 387 mm from Blaney-Criddle method) and closer in the month of February (1.34 mm from the H–S method). The reason for the large difference in August is due to the increased vegetation density during this peak growth period of pistachio trees and

grapes. Hence, increased actual ET due to increased growth and irrigation increased the gap between actual and potential ET in the arid region (Table 2).

Comparison of ET_0 from the empirical models against the FAO PM method suggests that H–S, Blaney-Criddle and Trabert may be the most suitable models among the ten models. On the other hand, Trajkovic, Bereti, Tabari, and Droogers-Allen models were identified as the unsuitable methods with large MAE and RMSE. As expected, MAE of ET_0 from all models were maximum during the month of August and minimum in February (Table 3).

MAE values increased which slightly increased during the month of November and were highest for the month of August (Fig. 9).

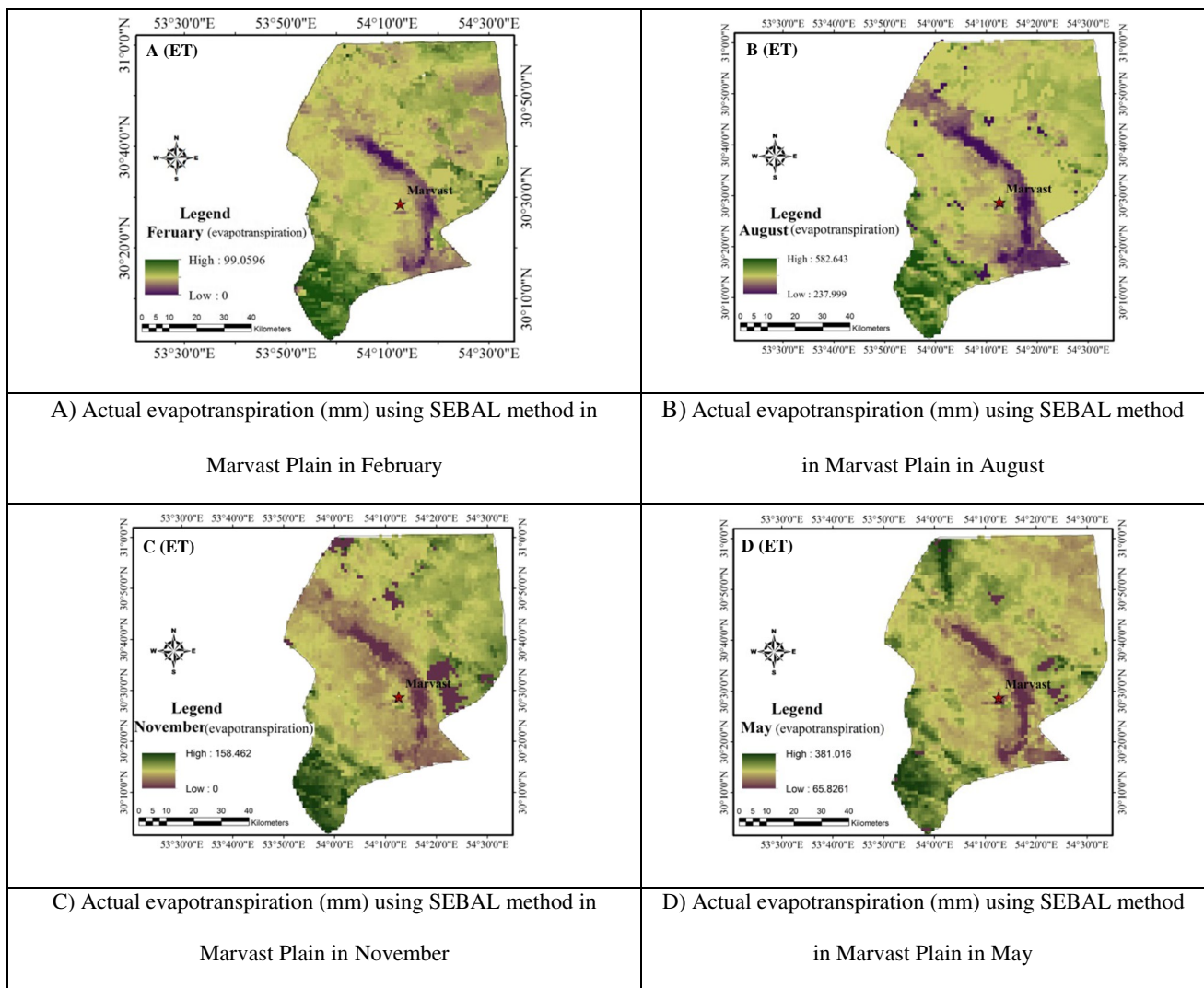


Fig. 7 Actual evapotranspiration (mm) using SEBAL method in Marvast Plain in February, August, November, and May for the period 2017

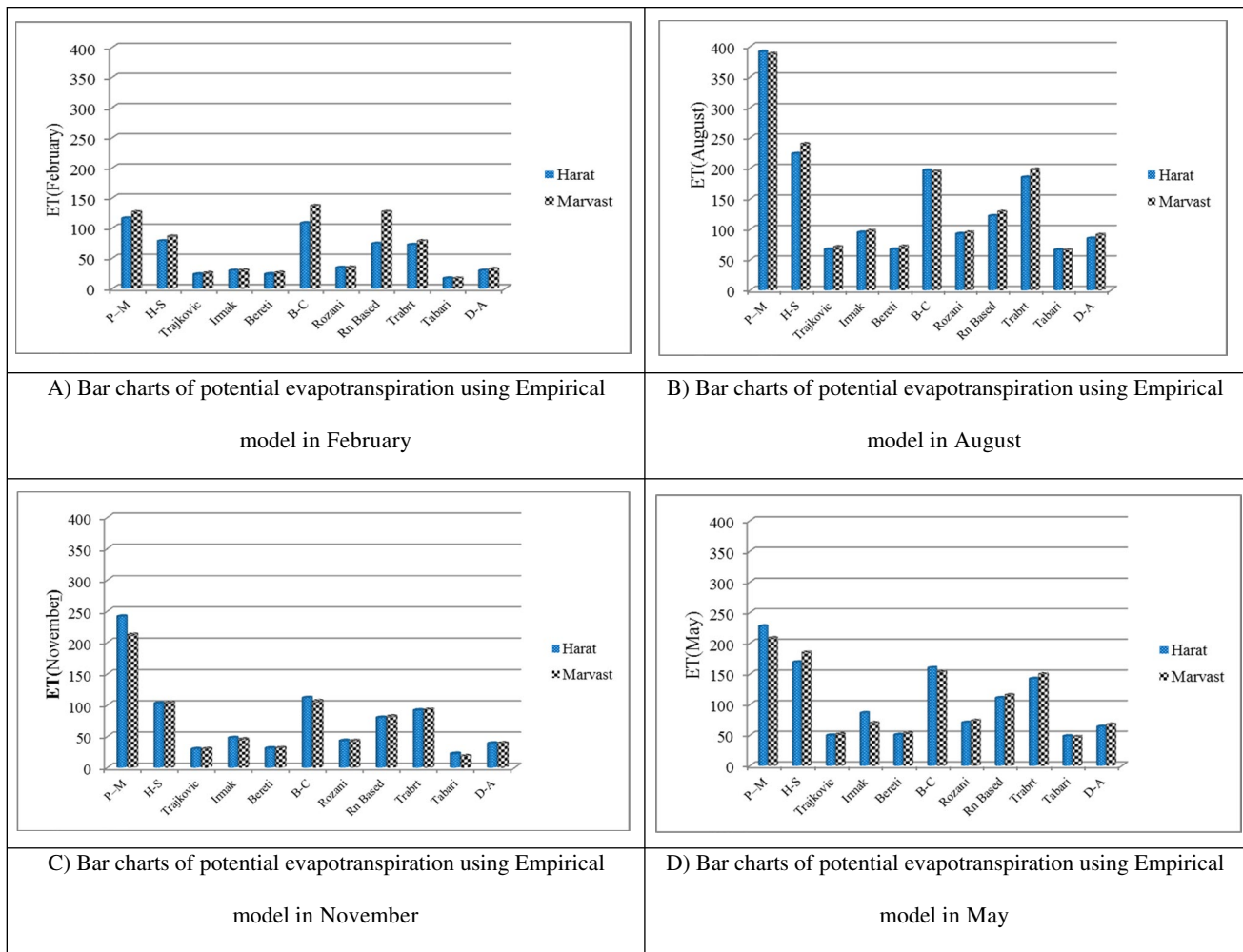


Fig. 8 Bar charts of potential evapotranspiration using empirical model

Table 2 Estimation of monthly evapotranspiration using experimental methods and estimates by SEBAL algorithm (absolute difference) (mm)

Herat plain		MAE				Marvast plain		MAE			
Models	August	February	May	November	Models	August	February	May	November		
Trajkovic	485.79	53.67	272.99	131.04	Trajkovic	510.8	73.6	329.2	128.5		
Irmak	458.11	47.73	236.49	113.08	Irmak	484.4	69.0	310.9	112.7		
Bereti	485.77	53.41	272.03	129.73	Bereti	510.0	73.2	327.4	126.9		
Blaney-Criddle	356.45	31.00	162.80	48.86	blaney criddle	387.0	37.0	227.8	51.6		
Rozani	460.27	42.75	252.11	117.60	Rozani	487.0	64.3	307.2	115.2		
Rn Based	430.84	2.78	211.74	80.61	Rn Based	453.1	27.9	265.3	76.0		
Trabert	367.92	4.78	180.31	68.94	Trabert	384.0	20.6	231.2	65.6		
Tabari	486.72	59.94	274.2	138.39	Tabari	516.0	82.2	333.8	139.8		
Droogers – Allen	467.84	47.65	258.8	121.80	Droogers – Allen	490.8	66.8	313.5	119.0		
FAO PM	161.46	39.29	95.02	80.99	FAO PM	194.1	27.0	172.6	54.2		
H–S	329.18	1.33	153.80	57.78	H–S	342.0	12.9	196.4	54.4		

Discussion

This study examined the evapotranspiration and water requirements by using MODIS images and empirical models in the Central basin of Iran. The results of the study can be represented in two separate sections. The first section relates to the comparison of the results Kc among the empirical models, and the second shows the results of the Error rates.

Results of water requirement calculation

Figure 10 shows the Kc values of pistachio and grapes plants for four months in 2017, estimated based on monthly ET using SEBAL and ET0 using FAO-PM and several empirical models. The Kc values for pistachio and grapes from the FAO-PM are well within the range of early, mid, and late season Kc values reported by FAO (<http://www.fao.org/3/x0490e/x0490e0b.htm>). However, when the empirical models were used, Kc values were significantly higher and, in most cases, unrealistic values (Kc values well over 1.5). The reason for this can be the temporal variability of ET due to the variability of the weather condition and the spatial variability due to hydrological characteristics of soil, and types and density of vegetations.

This is largely because of the significantly lower ET0 from the empirical methods. The H–S models could work well for estimating early and late season Kc for both crops (Tables 6 and 7), as estimated Kc are within 0.29 and 1.14 of those from the FAO-PM method. Overall, H–S method was found to be yield Kc values for pistachios that were most comparable with those from FAO PM methods, compared to the other nine empirical methods. For example, Kc values (H–S and FAO PM methods) were high in the early stages of plant growth, which is spring or May (1.50 and 1.11) and summer or August (1.64 and 0.9), respectively. Kc values (H–S and FAO PM methods) in the autumn (November 0.33 and 0.14) and winter (February 0.14 and 0.4) were low due to reduced growth of plants in these seasons (Fig. 10).

Similar to pistachio, Grape Kc values, from H–S method and FAO PM, were similar in the initial and late stages of the plant growth. The Peak season grape Kc values from the H–S method were 62% higher than those from FAO PM method, that is the closest value among all ten empirical models. Among other models, the Blaney-Criddle model yielded closest Kc values compared to the FAO PM method, expect for the month of August, when the estimated Kc values are 2.28 for the grape crop and 1.86 for the pistachio tree. While several models showed potential to produce reasonable Kc values for early and late seasons, all of them showed strong tendency to overestimate Kc values for the peak growing season. Few experimental methods, such as Trajkovic, Bereti, Droogers -Allen, and Tabari, produced

Table 3 The difference between the ET₀ from FAO PM and the empirical models (mm)

Crop	Month	FAO PM	Trajkovic	Irmak	Bereti	Blaney-Criddle	Rozani	Rn Based	Trabert	Tabari	Droogers—Allen	Har-greaves-Samani	MAE
Pistachio	August	391.4	324.3	296.7	324.3	195.0	298.8	269.4	206.5	325.3	306.4	167.7	
	February	116.2	93.0	87.0	92.7	8.0	82.0	42.1	44.1	99.2	86.9	38.0	
	May	227.7	178.0	141.5	177.0	67.8	157.1	116.7	85.3	179.2	163.8	58.8	
Grape	November	241.6	212.0	194.1	210.7	129.9	198.6	161.6	149.9	219.4	202.8	138.8	
	August	387.9	156.6	464.4	492.0	362.7	466.5	437.1	374.2	493.0	474.1	167.7	
	February	126.6	55.0	125.0	130.7	46.0	120.0	80.0	82.0	137.2	124.9	38.0	
	May	208.4	119.2	200.2	235.8	126.6	215.9	175.5	144.1	238.0	222.6	58.8	
	November	212.2	73.3	332.8	349.5	268.6	337.4	300.4	288.7	358.1	341.6	138.8	

Kc values that were well above 5. Especially most of these methods showed Kc values well above 1 for the grape product in February not for pistachio, which was closer to those from the FAO PM method. Overall, the Kc estimates from the experimental methods do not suggest a reasonable amount of water needs for pistachios and grapes, compared to FAO-PM method and FAO tables. However, H–S, Blaney-Criddle and Trabert showed an appropriate capability for early and late season estimations.

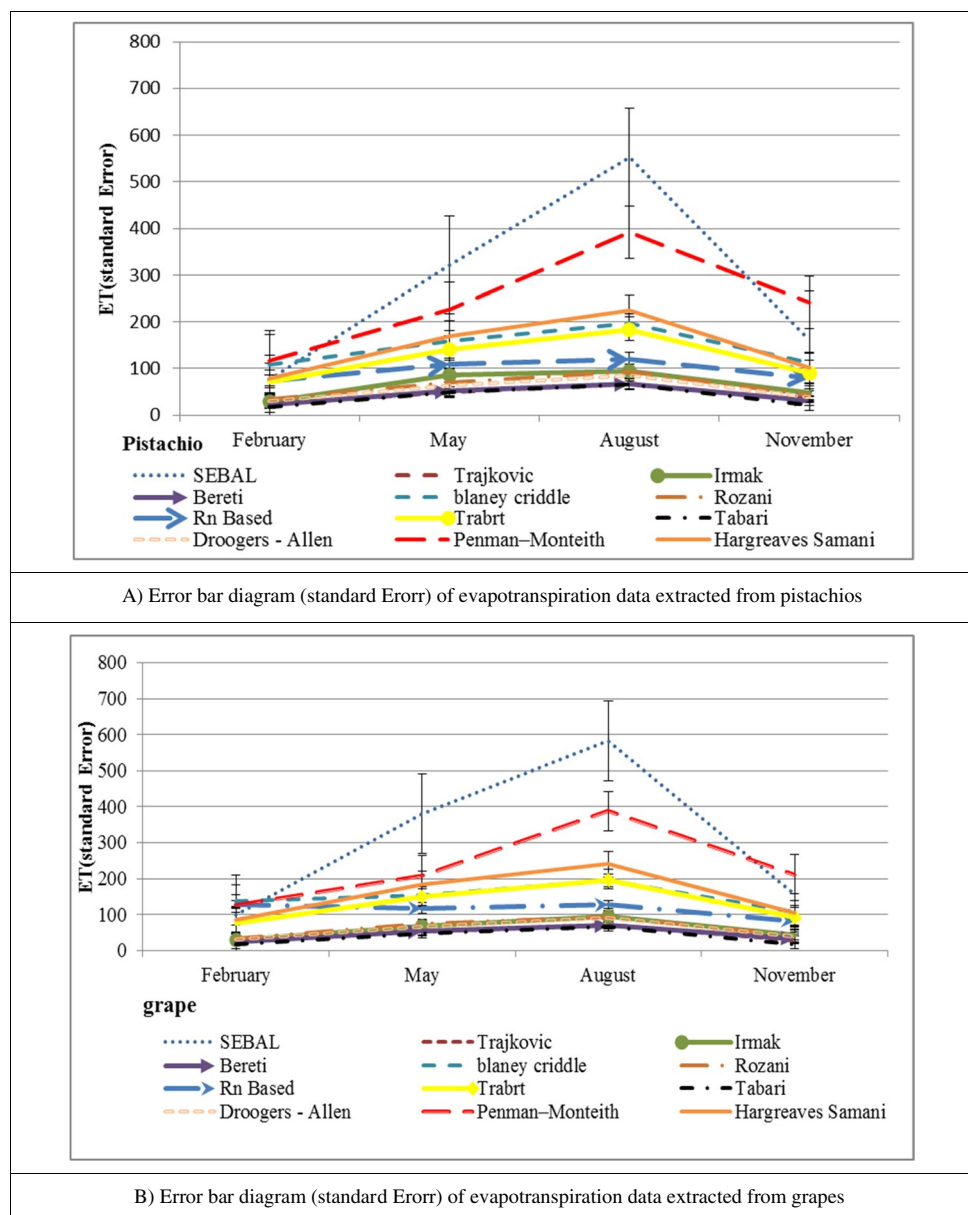
The lowest rate difference of Kc for pistachio from H–S and FAO PM was 0.05 in February and the highest difference Kc values were 0.70 in August. For the Kc values using the Blaney-Criddle method, the highest difference was 0.93 in August and the lowest in February (0.01). These values were slightly higher when Trabert method was used. Similar

results were obtained for grape Kc values. Several experimental methods, such as Trajkovic, Bereti, Irmak and Rozani methods, showed huge differences in Kc values, suggesting that these methods may not be applicable for estimating crop water requirements in these regions (Tables 4, 5, 6, and 7).

Conclusions

Desert and arid regions have a higher demand for ET and are expected to increase with climate change. Hence, available water resources, especially groundwater, are under pressure in these regions, as almost all of precipitation is lost through ET due to high temperature, low relative humidity, hot winds, significant sunlight, and sunshine, as well as the

Fig. 9 Error bar diagram (standard error) of evapotranspiration data extracted from two products, pistachios and grapes



low number of cloudy days. In several countries, the FAO-56 method based on the vegetation and meteorological parameters is used to estimate crop water requirement and Kc. Given the spatial variability of ET across space, especially

with variations in vegetation and meteorological parameters, it is not possible to calculate such parameters with a limited number of terrestrial and synoptic observations in data-poor regions like the Central basin of Iran. In this paper,

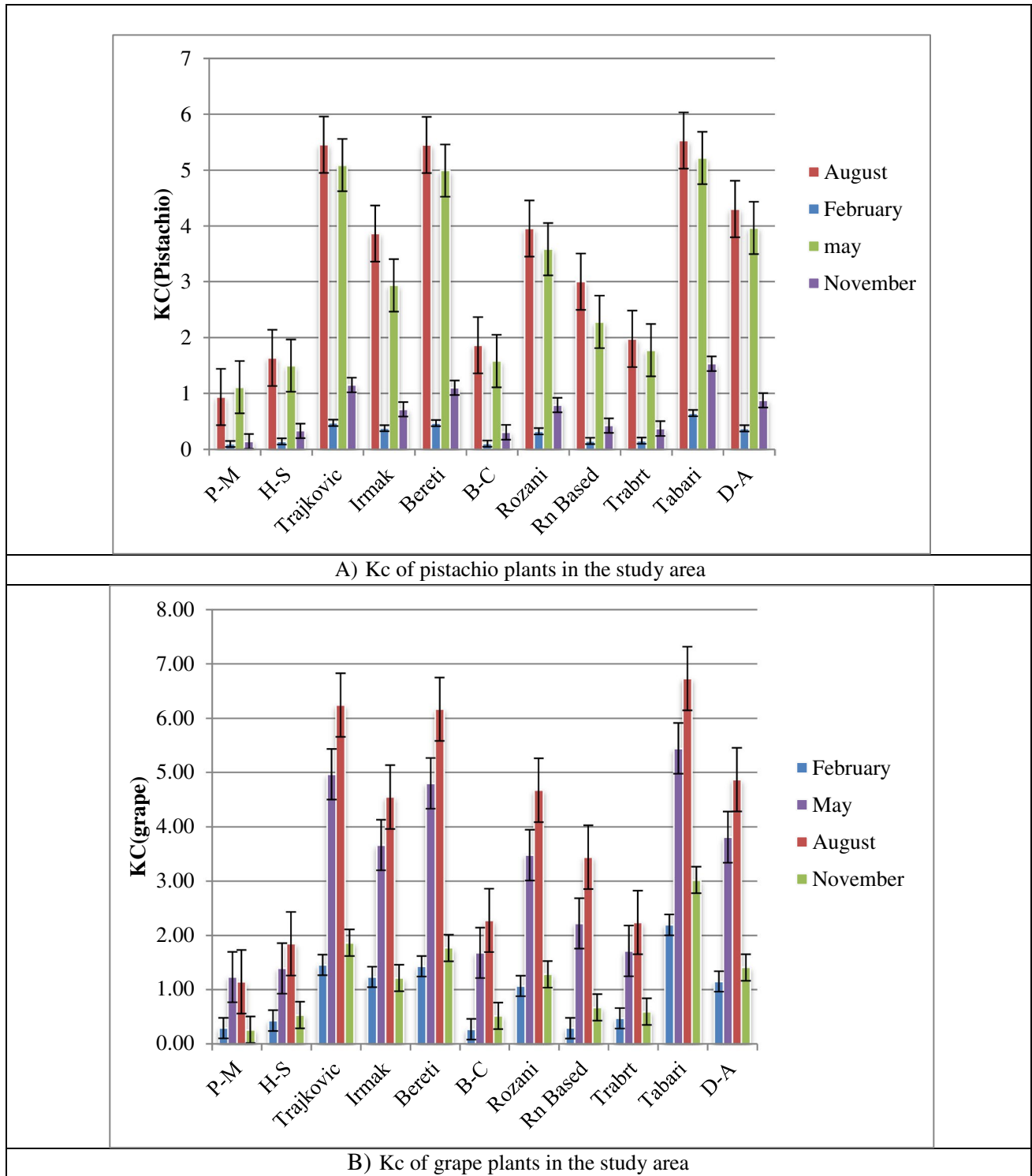


Fig. 10 Kc of pistachio and grape plants in the study area

Table 4 Pistachio K_C coefficient in different methods of evaporation transmittance and MAE coefficient

Methods	K _C				(MAE)			
	Month							
	February	August	November	May	February	August	November	May
FAO PM	0.094	0.93	0.14	1.11	-	-	-	-
Hargreaves-Samani	0.14	1.63	0.33	1.49	0.05	0.70	0.19	0.39
Trajkovic	0.47	5.45	1.15	5.08	0.38	4.52	1.01	3.98
Irmak	0.37	3.86	0.71	2.93	0.28	2.93	0.58	1.82
Bereti	0.46	5.45	1.10	4.99	0.37	4.52	0.96	3.88
Blaney-Criddle	0.10	1.86	0.30	1.58	0.01	0.93	0.16	0.47
Rozani	0.32	3.95	0.79	3.58	0.23	3.02	0.65	2.47
Rn-Based	0.14	2.99	0.42	2.27	0.05	2.06	0.28	1.17
Trabert	0.15	1.97	0.37	1.77	0.06	1.04	0.23	0.67
Tabari	0.64	5.53	1.53	5.21	0.55	4.60	1.39	4.11
Droogers – Allen	0.37	4.30	0.87	3.96	0.28	3.37	0.74	2.85

Table 5 Error rate of pistachio water requirement in experimental methods

Methods	H- S	Trajkovic	Irmak	Bereti	blaney criddle	Rozani	Rn Based	Trabert	Tabari	Droogers—Allen
RMSE	0.66	1.82	1.37	1.80	0.72	1.46	1.09	0.82	1.88	1.55

we overcame this challenge by using the SEBAL algorithm to estimate monthly ET for August, May, November, and February in 2017 using MODIS satellite images across the plains of Herat and Marvast in the Central basin of Iran. Monthly actual ET increased from spring to summer due to higher temperature, irrigation, and increased vegetation

growth pistachio orchards, grape orchards, agricultural lands, and forests.

The crop water requirements based on the widely regarded FAO PM method showed higher K_C values for grape and pistachio in August and lowest in February and November the K_C values from all 10 experimental methods

Table 6 Grape K_C coefficient in different methods of evaporation transmittance and MAE coefficient

Methods	K _C				(MAE)			
	Month							
	February	August	November	May	February	August	November	May
FAO PM	0.29	1.14	0.26	1.23	-	-	-	-
Hargreaves-Samani	0.43	1.85	0.53	1.39	0.14	0.71	0.27	0.16
Trajkovic	1.46	6.24	1.86	4.96	1.16	5.10	1.60	3.73
Irmak	1.23	4.55	1.21	3.67	0.94	3.41	0.96	2.43
Bereti	1.43	6.17	1.77	4.80	1.14	5.02	1.51	3.56
blaney criddle	0.27	2.28	0.52	1.68	0.02	1.13	0.26	0.44
Rozani	1.07	4.67	1.28	3.48	0.78	3.53	1.02	2.25
Rn Based	0.29	3.44	0.67	2.22	0.00	2.30	0.41	0.99
Trabert	0.47	2.24	0.60	1.72	0.18	1.10	0.34	0.48
Tabari	2.20	6.73	3.02	5.44	1.90	5.59	2.76	4.21
Droogers – Allen	1.15	4.87	1.41	3.81	0.86	3.72	1.15	2.58

Table 7 Error rate of grape water requirement in experimental methods

Methods	H-S	Trajkovic	Irmak	Bereti	blaney criddle	Rozani	Rn-Based	Trabert	Tabari	Droogers—Allen
RMSE	0.65	1.97	1.61	1.94	0.78	1.59	1.11	0.84	2.20	1.66

were significantly higher in August and the closet values were obtained from the H–S method. Results suggest that H–S, Blaney-Criddle, and Trabert models can produce comparable ET_0 and K_c values for estimating the pistachio and grape water requirements during early and late growing seasons. Other experimental methods, such as Trajkovic, Bereti, Droogers -Allen, and Tabari the amount of water required for pistachio trees in August and May, show very unrealistic values of K_c due to significantly low values of estimated ET_0 from these models. Results suggest that in our study area, H–S, Blaney-Criddle, and Trabert models have a better potential in terms of estimating the pistachio and grape water needs. On the other hand, Trajkovic, Bereti, and Rozani methods are not applicable, especially in August and May. Future study will cover more growing seasons and months and Landsat images to study crop water requirement at a plot scale.

Acknowledgements The authors would like to Thank, Dr Bhattarai Nishan from Michigan University for his valuable comments and suggestions, which helped to improve the paper.

Declarations

Conflict of interest The authors declare no competing interests.

References

- Allen RG, Pereira LS, Raes D, Smith M (1998) Crop Evapotranspiration Guidelines for computing crop water requirements. *FAO Irrig Drain* 56(3):1–300
- Allen RG, Tasumi M, Trezza R (2007) Satellite-based energy balance for mapping evapotranspiration with internalized calibration (METRIC)-model. *J Irrig Drain Eng* 133(4):380–394
- Amato U, Antoniadis A, Cuomo V, Cutillo L, Franzese M, Murino L, Serio C (2008) Statistical cloud detection from SEVIRI multispectral images. *Remote Sens Environ* 112(6):750–766
- Anderson MC, Norman JM, Kustas WP, Houborg R, Starks PJ, Agam N (2008) A thermal-based remote sensing technique for routine mapping of land-surface carbon, water and energy fluxes from field to regional scales. *Remote Sens Environ* 112(12):4227–4241
- Bashir Mohammed A, Tanakamaru H, Tada A (2010) Application of remote sensing for estimating crop water requirements, yield and water productivity of wheat in the Gezira Scheme. *Int J Remote Sens* 31(16):4281–4294
- Bastiaanssen WGM, Menenti M, Feddes RA, Holtslang AA (1998) Remote sensing surface energy balance algorithm for land (SEBAL): Formulation. *J Hydrol* 2(98):198–212
- Bastiaanssen WGM, Noordman EJM, Pelgrum H, Davids G (2005) SEBAL model with remotely sensed data to improve water-resources management under actual field conditions. *J Irrig Drain Eng* 131(85):85–93
- Bates B, Kundzewicz Z W, Palutikof J (2008) Climate change and water: technical paper VI. Intergovernmental Panel on Climate Change (IPCC), Geneva, Switzerland 3(12):1–20
- Bellvert J, Adeline K, Baram S, Pierce L, Sanden BL, Smart DR (2018) Monitoring crop evapotranspiration and crop coefficients over an almond and pistachio orchard throughout remote sensing. *Remote Sens* 10(12):1–22
- Bhattarai N, Liu T (2019) Land MOD ET mapper: a new matlab-based graphical user interface (GUI) for automated implementation of SEBAL and METRIC models in thermal imagery. *Environ Model Softw* 118(6):76–82
- Bhattarai N, Dougherty M, Marzen L, Kalin L (2012) Validation of evaporation estimates from a modified surface energy balance algorithm for land (SEBAL) model in the south-eastern United States. *Remote Sens Lett* 6(3):511–519
- Bhattarai N, Shaw SB, Quackenbush LJ, Im J, Niraula R (2016) Evaluating five remote sensing based single-source surface energy balance models for estimating daily evapotranspiration in a humid subtropical climate. *Int J Appl Earth Obs Geoinf* 49(10):75–86
- Bhattarai N, Mallick K, Stuart J, DuttVishwakarma B, Niraula R, Sen S, Jain M (2019) An automated multi-model evapotranspiration mapping framework using remotely sensed and reanalysis data. *Remote Sens Environ* 229(6):69–92
- Brutsaert W (2005) *Hydrology—An Introduction*. Press, Cambridge University
- Cai J, Liu Y, Lei T, Pereira LS (2007) Estimating reference evapotranspiration with the FAO Penman-Monteith equation using daily weather forecast messages. *Agric for Meteorol* 145(1):22–35
- Chartzoulakis K, Bertaki M (2015) Sustainable water management in agriculture under climate change. *J Agric Sci* 4(3):88–98
- Dehghanianij H, Oweis T, Sarwar Qureshi A (2006) Agricultural water use and management in arid and semiarid areas: current situation and measures for improvement. *Ann Arid Zone* 45(3):1–24
- Gao Y, Long D, Li Z (2008) Estimation of daily evapotranspiration from remotely sensed data under complex terrain over the upper Chao river basin in north China. *Int J Remote Sens* 29(11):3295–3315
- Gao X, Miao S, Luan Q, Zhao X, Wang J, He G, Zhao Y (2019) The spatial and temporal evolution of the actual evapotranspiration based on the remote sensing method in the Loess Plateau. *Sci Total Environ* 708(1):1–38
- Gocic M, Trajkovic S (2010) Software for estimating reference evapotranspiration using limited weather data. *Comput Electron Agric* 71(2):158–162
- Goldhamer DA (1995) Irrigation management. In: Ferguson L (ed) *Pistachio production*. Center for fruit and nut research and information, Davis CA 17(4):71–81
- Hyndman RJ, Koehler AB (2006) Another look at measures of forecast accuracy. *Int J Forecast* 22(4):679–688. <https://doi.org/10.1016/j.ijforecast.2006.03.001>
- Islam AE (2004) Real-time crop coefficient from SEBAL method for estimating the evapotranspiration. *SPIE Remote Sens* 5232(1):1–20. <https://doi.org/10.1117/12.510664>
- Jensen M (1968) *Water consumption by agricultural plants. Water Deficits and Plant Growth*. Academic Press, New York
- Li H, Zheng L, Lei Y, Li C, Liu Z, Zhang S (2008) Estimation of water consumption and crop water productivity of winter wheat in North China Plain using remote sensing technology. *Agric Water Manag* 95(11):1271–1277
- Mazidi A, Barzegar Marvasti Z (2016) Khatam tourism climate assessment (case study: Herat Station, Marvast, Khansar). *Gsonfkh01* (1):1–9
- Menenti M, Choudhury BJ (1993) Parameterization of land surface evapotranspiration using a location dependent potential evapotranspiration and surface temperature range. *H J Bolle* 212(7):561–568
- Moghim H, Zare Abadi Iqbal M (2014) Qualitative zoning of Herat aquifer (Yazd Spartina alterniflora in a simulated tidal system. *Environ Exp Bot* 58:140–148
- Piri H, Taher M (2019) Evaluation of 24 models of reference plant evaporation and transpiration in different climates of Iran. *I J Eco Hydrol* 6(3):611–622

- Rahimzadegan M, Janani A (2019) Estimating evapotranspiration of pistachio crop based on SEBAL algorithm using Landsat 8 satellite imagery. *Agric Water Manag* 217(1):383–390
- Rawat KS, Bala A, Kumar Singh S, Pal RK (2017) Quantification of wheat crop evapotranspiration and mapping: a case study from Bhiwani District of Haryana India. *Agric Water Manag* 187(4):200–209
- Ray DK, Mueller ND, West PC, Foley JA (2013) Yield trends are insufficient to double global crop production by 2050. *PLoS One* 8(6):66428–66438. <https://doi.org/10.1371/journal.pone.0066428>
- Su Z (2002) The Surface Energy Balance System (SEBS) for estimation of turbulent heat fluxes. *Hydrol Earth Syst Sci* 6(1):85–99
- Tabari H, Hosseinzadeh Talaei P (2011) Local calibration of the Hargreaves and Priestley-Taylor equations for estimating reference evapotranspiration in arid and cold climates of Iran based on the Penman-Monteith model. *J Hydrol Eng ASCE* 16(10):1–10. [https://doi.org/10.1061/\(ASCE\)HE.1943-5584.0000366](https://doi.org/10.1061/(ASCE)HE.1943-5584.0000366)
- Tabari H, Grismer ME, Trajkovic S (2011) Comparative analysis of 31 reference evapotranspiration methods under humid conditions. *Irrig Sci* 1(31):107–117
- Tang R, Liang Z, Li KSC, Jia Y, Li C, Sun X (2013) Spatial-scale effect on the SEBAL model for evapotranspiration estimation using remote sensing data. *Agric for Meteorol* 174(15):28–42
- Wan Z (2014) New refinements and validation of the collection-6 MODIS land-surface temperature/emissivity product. *Remote Sens Environ* 140(1):36–45
- Waters R, Allen R, Tasumi M, Trezza R, Bastiaanssen W (2002a) SEBAL, Advanced Training and User's Manual. Idaho Implementation 1(1):1–97
- Waters R, Allen R, Bastiaanssen W, Tasumi M, Trezza R (2002b) Surface energy balance algorithms for Land Idaho Implementation Advanced Training and User's Manual. Idaho Implementation 1(2):1–97
- Yamaç SS, Todorovic M (2019) Estimation of daily potato crop evapotranspiration using three different machine learning algorithms and four scenarios of available meteorological data. *Agric Water Manag* 228(1):1–12
- Yanga Y, Andersona MC, Gaoa F, Wardlowb B, Hain CR, Otkin JA, Alfieri J, Yang Y, Sun L, Dulaney W (2018) Field-scale mapping of evaporative stress indicators of crop yield: an application over Mead, NE, USA. *Remote Sens Environ* 210(2):387–402

Springer Nature or its licensor holds exclusive rights to this article under a publishing agreement with the author(s) or other rightsholder(s); author self-archiving of the accepted manuscript version of this article is solely governed by the terms of such publishing agreement and applicable law.